Plan

- 6.7. Contacts Conditions
- 6.7.1. Continuum Mechanics Equations
- 6.7.2. A Solution Approach for Contact Problems : The Constraints Function Method

- 6.8. Some practical considerations
- 6.8.1. The general Approach to Nonlinear Analysis
- 6.8.2. Collapse and Buckling Analyses
- 6.8.3. The Effects of Elements Distortions
- 6.8.4. The Effects of Order of Numerical Integration

- Exercice 6.24
- Exercice 6.27

6.7. Contacts Conditions

- Difficult non linear behavior = contact between two or more bodies
- Contacts = From frictionless in small displacement to friction in general strain
- Nonlinearity of the analysis is not only geometric and material but also contact conditions

Objective

- Briefly state the contact conditions in the context of finite element analysis and present a general approach for solution

6.7.1. Continuum Mechanics Equations

We consider N bodies that are in contact at time t

S_c is the complete area of contact

${}^tf_i^C$: Components of contact tractions

${}^tf_i^S$: components of the known externally applied traction

Concept of virtual work for the N bodies at time t

$$\sum_{L=1}^{N}\left\{\int_{{}^tV} {}^t\tau_{ij}\,\delta_t e_{ij}\,d^tV\right\} = \underbrace{\sum_{L=1}^{N}\left\{\int_{{}^tV}\delta u_i\,{}^tf_i^B\,d^tV + \int_{{}^tS_f}\delta u_i^S\,{}^tf_i^S\,d^tS\right\}}_{\text{Usual term}} + \underbrace{\sum_{L=1}^{N}\int_{{}^tS_c}\delta u_i^c\,{}^tf_i^c\,d^tS}_{\text{Contribution of contact forces}} \qquad (6.301)$$

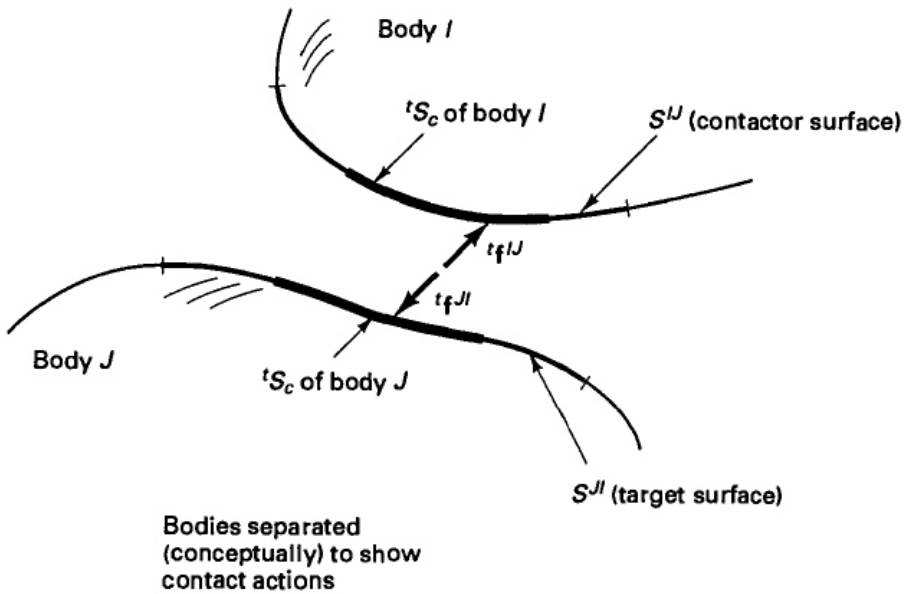

Figure 6.17 Bodies in contact at time t

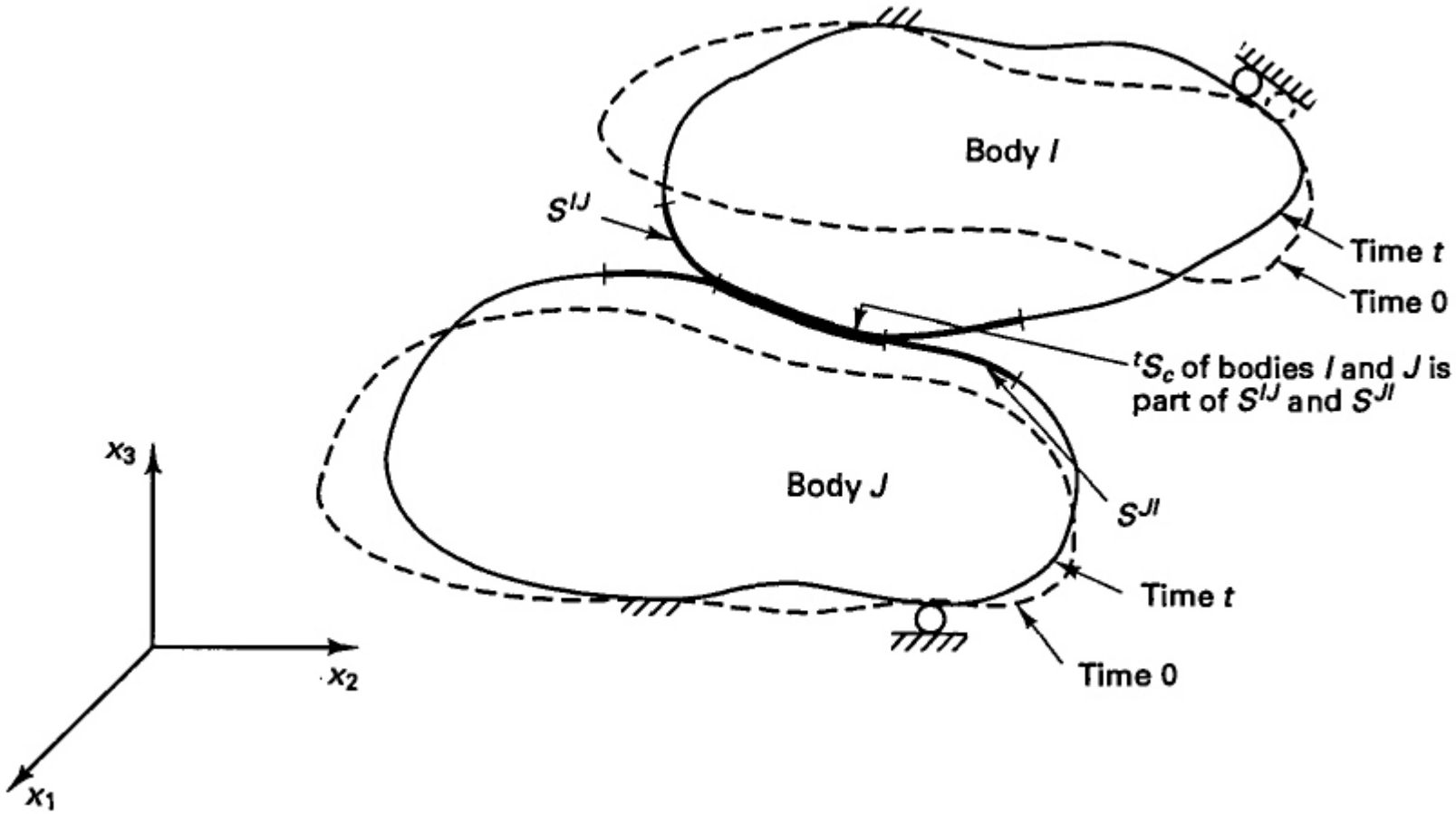

We denote 2 body I and J

Each body is supported such that without contact no rigid motion is possible

${}^t\mathbf{f}^{IJ}$: vector of contact surface traction on body I due to contact with body J then ${}^t\mathbf{f}^{IJ} = - {}^t\mathbf{f}^{JI}$

The virtual work due to the contact traction can be written :

$$\int_{S^{IJ}} \delta u_i^I \, {}^t f_i^{IJ} \, dS^{IJ} + \int_{S^{JI}} \delta u_i^I \, {}^t f_i^{JI} \, dS^{JI} = \int_{S^{IJ}} \delta u_i^{IJ} \, {}^t f_i^{IJ} \, dS^{IJ} \qquad (6.302)$$

We call pair of surface S^{IJ} and S^{JI}

- S^{IJ} : Contractor surface
- S^{JI} : Target surface

$$\int_{S^{IJ}} \delta u_i^I \, {}'f_i^{IJ} \, dS^{IJ} + \int_{S^{JI}} \delta u_i^J \, {}'f_i^{JI} \, dS^{JI} = \int_{S^{IJ}} \delta u_i^{IJ} \, {}'f_i^{IJ} \, dS^{IJ} \qquad (6.302)$$

Virtual work that the contact tractions produce
Over the virtual relative displacement
On the contact pair

Analyzes of the right-hand side

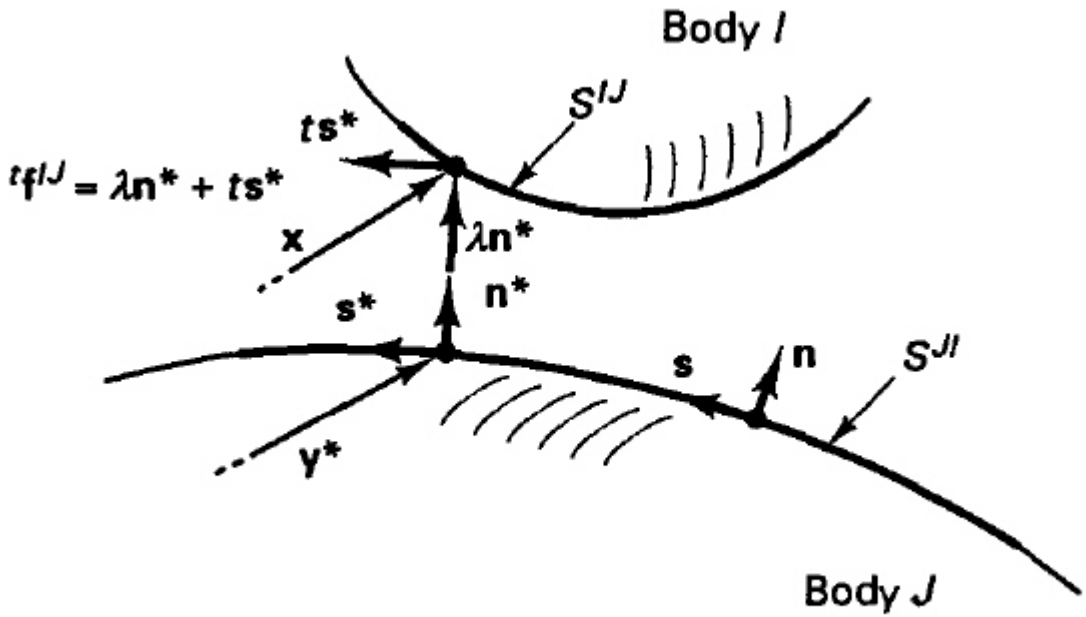

Figure 6.18 Definitions used in contact analysis

n : Unit outward normal to S^{IJ}

s : Unit vector

Decomposition of the contact traction ${}^tF^{IJ}$

$$'\mathbf{f}^{IJ} = \lambda \mathbf{n} + t\mathbf{s} \qquad (6.304$$

$$\lambda = ({}^{t}\mathbf{f}^{IJ})^{T}\mathbf{n}; \qquad t = ({}^{t}\mathbf{f}^{IJ})^{T}\mathbf{s} \tag{6.305}$$

x : generic point on S^{IJ}
y*(x,t) is the point on S^{JI} satisfying

$$\| \mathbf{x} - \mathbf{y}^{*}(\mathbf{x}, t) \|_2 = \min_{\mathbf{y} \in S^{JI}} \{ \| \mathbf{x} - \mathbf{y} \|_2 \} \tag{6.306}$$

The distance from x to S^{JI} is given by :

$$g(\mathbf{x}, t) = (\mathbf{x} - \mathbf{y}^{*})^{T}\mathbf{n}^{*} \tag{6.307}$$

Where **n*** is the unit “normal vector” that we use at **y*(x,t)**
The function g is the gap function for the contact surface pair

The conditions for normal contact can be written as :

$$g \geq 0; \qquad \lambda \geq 0; \qquad g\lambda = 0 \tag{6.308}$$

Express the fact that if g >0 we must have λ = 0

Let us define the nondimensional variable τ given by

$$\tau = \frac{t}{\mu\lambda} \qquad (6.309)$$

Frictional resistance

Magnitude of the relative tangential velocity corresponding to the unit tangential vector **s** at **y*(x,t)**

$$\dot{u}(\mathbf{x}, t) = (\dot{\mathbf{u}}^{J}|_{\mathbf{y}^*(\mathbf{x},t)} - \dot{\mathbf{u}}^{I}|_{(\mathbf{x},t)}) \cdot \mathbf{s}^* \qquad (6.310)$$

$\dot{u}(\mathbf{x}, t)\mathbf{s}^*$ Tangential velocity at time t of the material point at **y* relative to The material point at x**

Definitions Coulomb's law of friction states :

$$\left.\begin{aligned} & |\tau| \leq 1 \\ \text{and} \quad & |\tau| < 1 \text{ implies } \dot{u} = 0 \\ \text{while} \quad & |\tau| = 1 \text{ implies sign } (\dot{u}) = \text{sign } (\tau) \end{aligned}\right\} \tag{6.311}$$

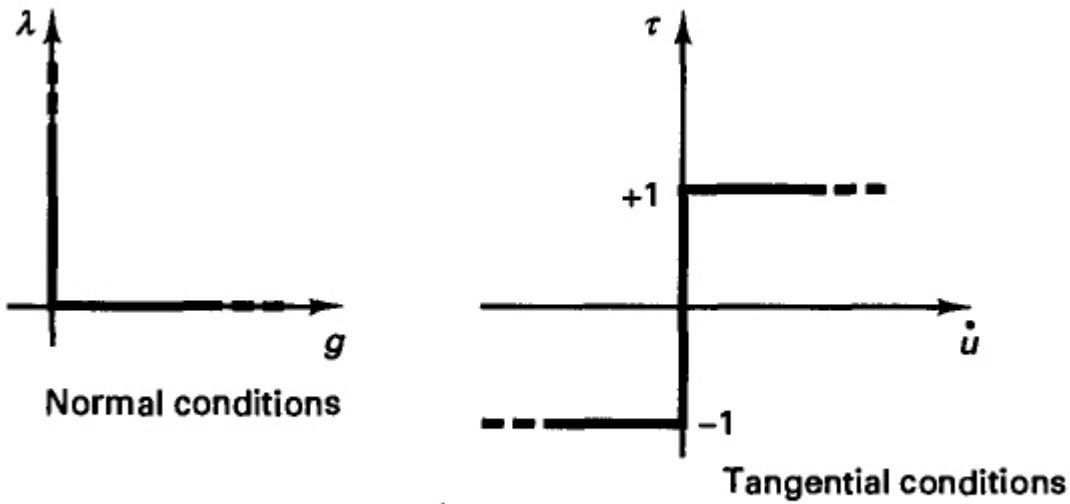

Figure 6.19 Interface conditions in contact analysis

- Previous example consider pseudo-staic contact condition
- In dynamic analysis:

Body forces mean Inertial force effect + kinematic interface conditions must be satisfied at all instances of time required displacement, velocity and acceleration compatibility between the contacting bodies.

Various algorithms have been proposed to solve contact problems in Finite Element analysis.

6.7.2. A Solution Approach for Contact Problems : The Constraints Function Method

- w is a function of g and λ that satisfied $w(g, \lambda) = 0$

and $g \geq 0; \qquad \lambda \geq 0; \qquad g\lambda = 0$ (6.308)

- τ and $\dot{u}$ such that the solutions of $v(\dot{u}, \tau) = 0$

Then contact conditions are given by

$$w(g, \lambda) = 0 \tag{6.312}$$

$$v(\dot{u}, \tau) = 0 \tag{6.313}$$

Multiplying (6.312) by $\delta\lambda$ and (6.313) by $\delta\tau$ and integrating over S^{IJ}, we obtain the constraint equation

$$\int_{S^{IJ}} [\delta\lambda\, w(g, \lambda) + \delta\tau\, v(\dot{u}, \tau)]\, dS^{IJ} = 0 \tag{6.314}$$

In summary, the governing equations to be solved for the two-body contact problem in Fig. 6.17 are the usual principle of virtual work equation, with the effect of the contact tractions included through externally applied (but unknown) forces, plus the constraint equation (6.314). Of course, the principle of virtual work (6.301) is in the two-body contact problem specialized to bodies I and J only, and the contact force term is given by (6.302) and (6.303).

The finite element solution of the governing continuum mechanics equations is obtained by using the discretization procedures for the principle of virtual work, and in addition now discretizing the contact conditions also.

Example on the formulation governing finite element equation

We consider two-dimensional case of contractor and target bodies:
Node k1 and k2 define straight boundary but not necessary corner node of an element

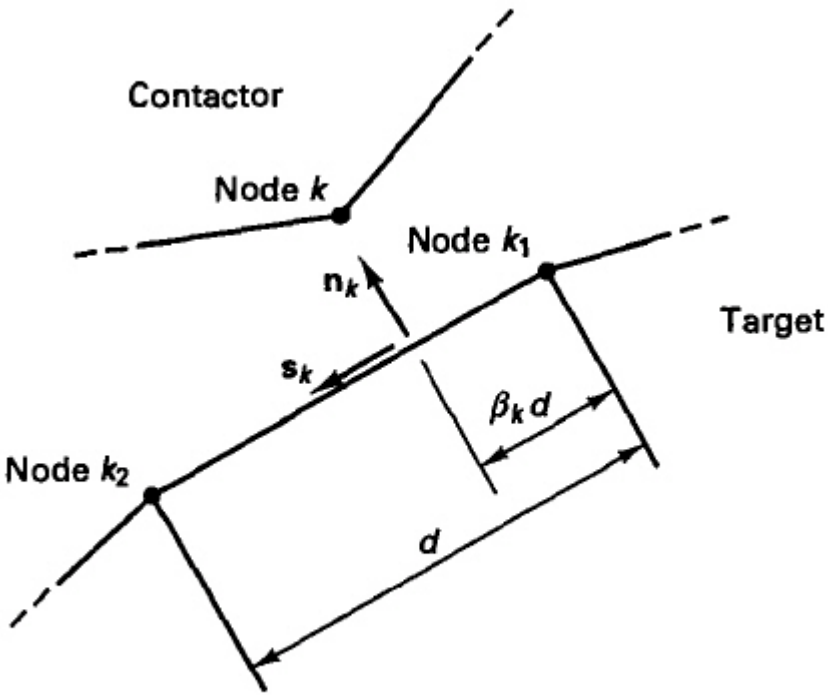

Figure 6.20 Two-dimensional case of contact

- Discretization of the continuum equations 6.301 and 6.314 at time t+Δt gives :

$$\sum_{L=1}^{N} \left\{ \int_{{}^{t}V} {}^{t}\tau_{ij}\, \delta_t e_{ij}\, d^{t}V \right\} = \sum_{L=1}^{N} \left\{ \int_{{}^{t}V} \delta u_i\, {}^{t}f_i^B\, d^{t}V + \int_{{}^{t}S_f} \delta u_i^S\, {}^{t}f_i^S\, d^{t}S \right\} + \sum_{L=1}^{N} \int_{{}^{t}S_c} \delta u_i^c\, {}^{t}f_i^c\, d^{t}S \qquad (6.301)$$

$$\int_{S^{IJ}} [\delta\lambda\, w(g, \lambda) + \delta\tau\, v(\dot{u}, \tau)]\, dS^{IJ} = 0 \qquad (6.314)$$

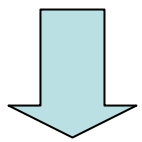

$$ {}^{t+\Delta t}\mathbf{F}({}^{t+\Delta t}\mathbf{U}) = {}^{t+\Delta t}\mathbf{R} - {}^{t+\Delta t}\mathbf{R}_c({}^{t+\Delta t}\mathbf{U}, {}^{t+\Delta t}\boldsymbol{\tau}) \qquad (6.315)$$

and

$$ {}^{t+\Delta t}\mathbf{F}_c({}^{t+\Delta t}\mathbf{U}, {}^{t+\Delta t}\boldsymbol{\tau}) = \mathbf{0} \qquad (6.316)$$

where with m contactor nodes,

$$ {}^{t+\Delta t}\boldsymbol{\tau}^T = [\lambda_1, \tau_1, \ldots, \lambda_k, \tau_k, \ldots, \lambda_m, \tau_m] \qquad (6.317)$$

The vector ${}^{t+\Delta t}\mathbf{R}_c$ is obtained by assembling for all m contactor nodes, $k = 1, \ldots, m$,

- The nodal force vector is

$$ {}^{t+\Delta t}\mathbf{R}_k^c = \begin{bmatrix} -\lambda_k(\mathbf{n}_k + \mu\tau_k \mathbf{s}_k) \\ (1 - \beta_k)\lambda_k(\mathbf{n}_k + \mu\tau_k \mathbf{s}_k) \\ \beta_k \lambda_k(\mathbf{n}_k + \mu\tau_k \mathbf{s}_k)] \end{bmatrix} \tag{6.318} $$

The vector ${}^{t+\Delta t}\mathbf{F}_c$ can be written as

$$ {}^{t+\Delta t}\mathbf{F}_c^T = [{}^{t+\Delta t}\mathbf{F}_1^{cT}, \ldots, {}^{t+\Delta t}\mathbf{F}_m^{cT}] \tag{6.319} $$

where

$$ {}^{t+\Delta t}\mathbf{F}_k^c = \begin{bmatrix} w(g_k, \lambda_k) \\ v(\dot{u}_k, \tau_k) \end{bmatrix} \tag{6.320} $$

Section 6.3.1, the resulting equations corresponding to the linearization about the state at time t are

$$\begin{bmatrix} ({}^t\mathbf{K} + {}^t\mathbf{K}^c_{uu}) & {}^t\mathbf{K}^c_{u\tau} \\ {}^t\mathbf{K}^c_{\tau u} & {}^t\mathbf{K}^c_{\tau\tau} \end{bmatrix} \begin{bmatrix} \Delta\mathbf{U} \\ \Delta\boldsymbol{\tau} \end{bmatrix} = \begin{bmatrix} {}^{t+\Delta t}\mathbf{R} - {}^t\mathbf{F} - {}^t\mathbf{R}_c \\ -{}^t\mathbf{F}_c \end{bmatrix} \tag{6.321}$$

where $\Delta\mathbf{U}$ and $\Delta\boldsymbol{\tau}$ are the increments in the solution variables ${}^t\mathbf{U}$ and ${}^t\boldsymbol{\tau}$, and ${}^t\mathbf{K}^c_{uu}$, ${}^t\mathbf{K}^c_{u\tau}$, ${}^t\mathbf{K}^c_{\tau u}$, and ${}^t\mathbf{K}^c_{\tau\tau}$ are contact stiffness matrices,

$$\left.\begin{aligned} {}^t\mathbf{K}^c_{uu} &= \frac{\partial {}^t\mathbf{R}_c}{\partial {}^t\mathbf{U}}; \qquad {}^t\mathbf{K}^c_{u\tau} = \frac{\partial {}^t\mathbf{R}_c}{\partial {}^t\boldsymbol{\tau}} \\ {}^t\mathbf{K}^c_{\tau u} &= \frac{\partial {}^t\mathbf{F}_c}{\partial {}^t\mathbf{U}}; \qquad {}^t\mathbf{K}^c_{\tau\tau} = \frac{\partial {}^t\mathbf{F}_c}{\partial {}^t\boldsymbol{\tau}} \end{aligned}\right\} \tag{6.322}$$

Conclusion

- Continuum mechanics formulation in section 6.7.1 has been given for very general conditions deformation and constitutive law.
- Formulation is applicable to frictionless contact

$$\begin{bmatrix} ({}^t\mathbf{K} + {}^t\mathbf{K}^c_{uu}) & {}^t\mathbf{K}^c_{u\tau} \\ {}^t\mathbf{K}^c_{\tau u} & {}^t\mathbf{K}^c_{\tau\tau} \end{bmatrix} \begin{bmatrix} \Delta\mathbf{U} \\ \Delta\boldsymbol{\tau} \end{bmatrix} = \begin{bmatrix} {}^{t+\Delta t}\mathbf{R} - {}^t\mathbf{F} - {}^t\mathbf{R}_c \\ -{}^t\mathbf{F}_c \end{bmatrix} \tag{6.321}$$

- 6.231 correspond to a full linearization.

If too large time step → Convergence difficulties because predicted intermediate state are too far from the solution.

6.8. Some practical considerations

The establishment of an appropriate mathematical model for the analysis of an engineering problem is to a large degree based on sufficient understanding of the problem under consideration and a reasonable knowledge of the finite element procedures available for solution (see Section 1.2). This observation is particularly applicable in nonlinear analysis because the appropriate nonlinear kinematic formulations, material models, and solution strategies need to be selected.

The objective in this section is to discuss briefly some important practical aspects pertaining to the selection of appropriate models and solution methods for nonlinear analysis.

6.8.1. The general Approach to Nonlinear Analysis

- Good practice in engineering analysis :

Nonlinear analysis always preceded by linear analysis so that the non linear analysis is an extension of the complete analysis beyond the assumptions of linear analysis.

The advantages of starting with a linear analysis after which judiciously selected nonlinear analyses are performed are that, first, the effect of each nonlinearity introduced can more easily be explained, second, confidence in the analysis results can be established and, third, useful information is accumulated throughout the period of analysis.

… In addition to general recommendations, practical aspects can be important :

6.8.2. Collapse and Buckling Analyses

Illustration of response structure when collapse or buckling

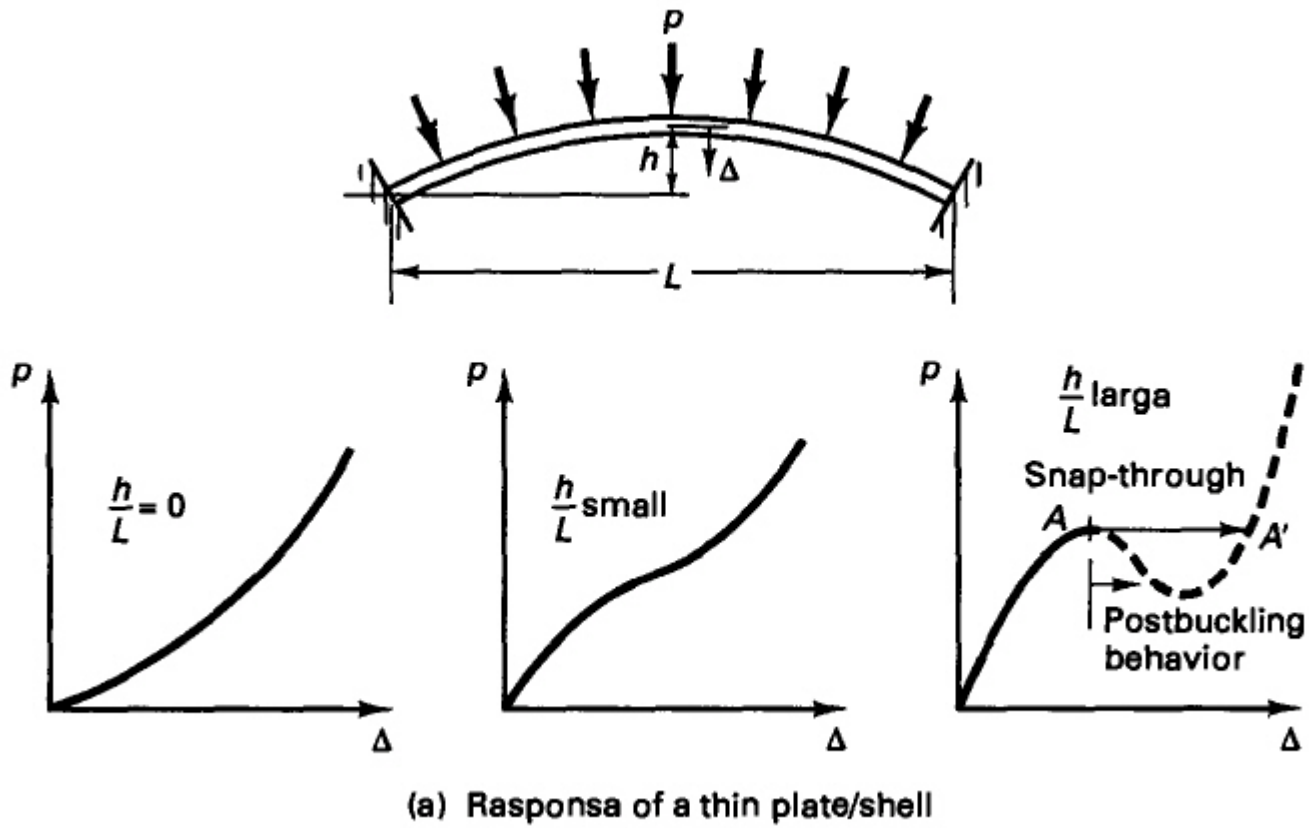

(a) Rasponsa of a thin plate/shell

Arch

After A :Post buckling (deformation) behavior, iduce by load increase = dynamic response

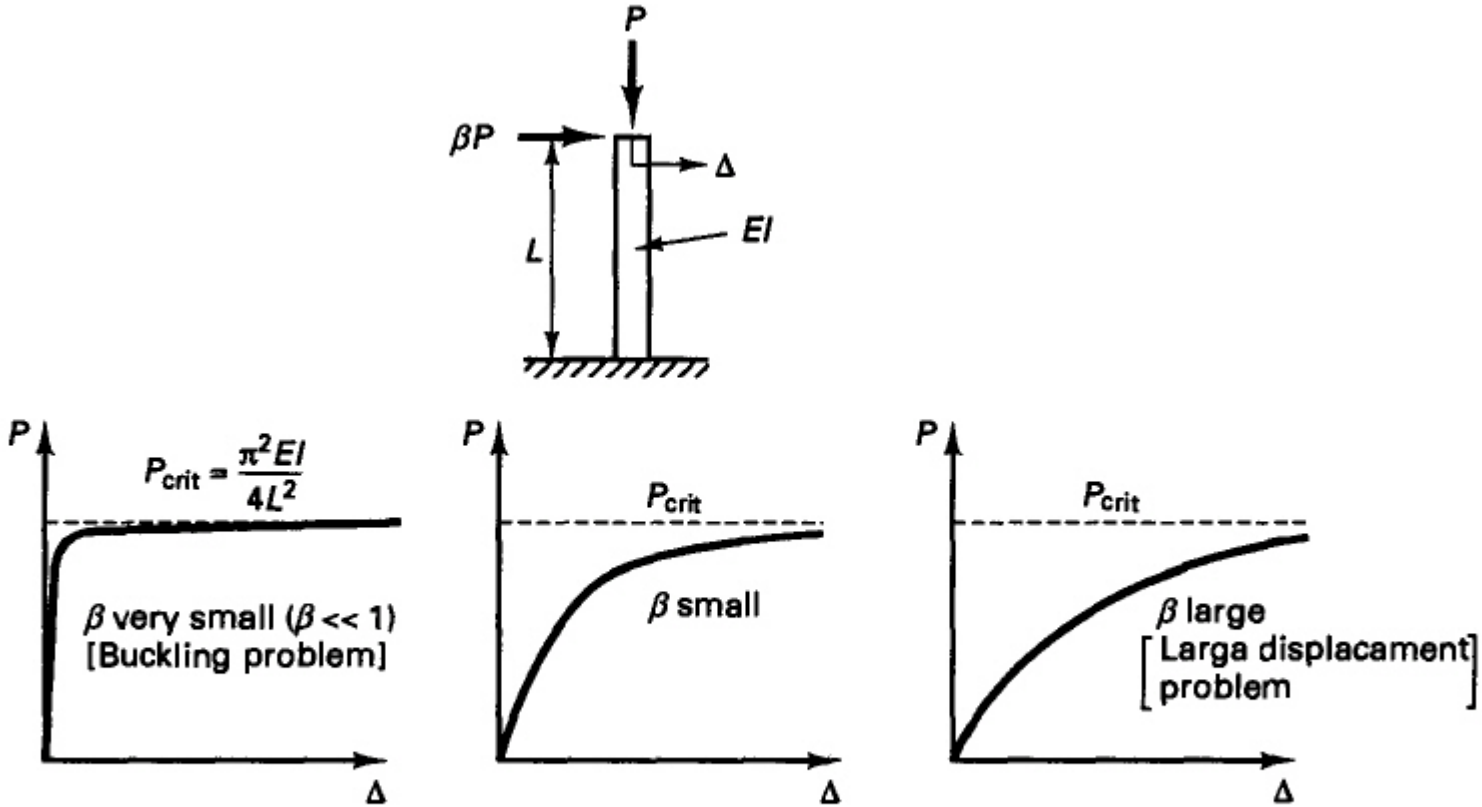

(b) Rasponse of a column

Figure 6.21 Instability and collapse analyses

The response of the column depend of β

When β is very small we are closed to a perfectly straigth column with only compressive load.

We consider the calculation of the linearized buckling load

- ${}^{t-\Delta t}K$ and ${}^{t}K$ stiffness matrix at time t-Δt and t
- ${}^{t-\Delta t}R$ and ${}^{t}R$ Vectors of externally applied load

We assume at any time τ

$$ {}^{\tau}\mathbf{K} = {}^{t-\Delta t}\mathbf{K} + \lambda({}^{t}\mathbf{K} - {}^{t-\Delta t}\mathbf{K}) \qquad (6.323) $$

$$ {}^{\tau}\mathbf{R} = {}^{t-\Delta t}\mathbf{R} + \lambda({}^{t}\mathbf{R} - {}^{t-\Delta t}\mathbf{R}) \qquad (6.324) $$

λ : Scaling factor

At collapse or buckling, the stiffness matrix is singular and the condition to calculate λ is

$$\det {}^{\tau}\mathbf{K} = 0 \tag{6.325}$$

or, equivalently (see Section 10.2),

$${}^{\tau}\mathbf{K}\boldsymbol{\phi} = \mathbf{0} \tag{6.326}$$

where $\boldsymbol{\phi}$ is a nonzero vector. Substituting from (6.323) into (6.326), we obtain the eigenproblem

$${}^{t-\Delta t}\mathbf{K}\boldsymbol{\phi} = \lambda({}^{t-\Delta t}\mathbf{K} - {}^{t}\mathbf{K})\boldsymbol{\phi} \tag{6.327}$$

Φ is a non zero vector

$$\boxed{{}^{\tau}\mathbf{K} = {}^{t-\Delta t}\mathbf{K} + \lambda({}^{t}\mathbf{K} - {}^{t-\Delta t}\mathbf{K})} \tag{6.323}$$

$$\boxed{{}^{t}\mathbf{K}\boldsymbol{\phi} = \gamma\,{}^{t-\Delta t}\mathbf{K}\boldsymbol{\phi}} \tag{6.328}$$

where

$$\gamma = \frac{\lambda - 1}{\lambda} \tag{6.329}$$

We are only interested in the only smallest positive eigenvalues, so;

$$\boxed{{}^{t}\mathbf{K}\boldsymbol{\phi} = \gamma\,{}^{t-\Delta t}\mathbf{K}\boldsymbol{\phi}} \tag{6.328}$$

where

$$\gamma = \frac{\lambda - 1}{\lambda} \tag{6.329}$$

Having evaluated γ_1, we obtain λ_1 from (6.329), and then the buckling (or collapse) load is given by (6.324),

$$\boxed{\mathbf{R}_{\text{buckling}} = {}^{t-\Delta t}\mathbf{R} + \lambda_1({}^{t}\mathbf{R} - {}^{t-\Delta t}\mathbf{R})} \tag{6.330}$$

The assumption used in the linearized buckling analysis are displayed in 6.323 and 6.324

$$ {}^{\tau}\mathbf{K} = {}^{t-\Delta t}\mathbf{K} + \lambda({}^{t}\mathbf{K} - {}^{t-\Delta t}\mathbf{K}) \qquad (6.323) $$

$$ {}^{\tau}\mathbf{R} = {}^{t-\Delta t}\mathbf{R} + \lambda({}^{t}\mathbf{R} - {}^{t-\Delta t}\mathbf{R}) \qquad (6.324 $$

We assume that the elements in the stiffness matrix vary lineary from time t-Δt onward
The slope of the change are being given by the difference from time t-Δt to time t.
The linearized buckling analysis gives a reasonable estimate of the collapse load only
If the the precollapse displacement are relatively small

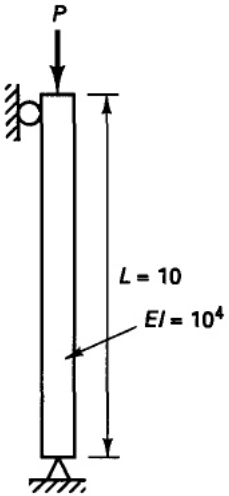

P_{cr} of mathematical model (analytical solution) = 986.96
P_{cr} of finite element model = 986.212 (for $^{\Delta t}P$ = 1, 10, and 100)

(a) Linearized buckling analysis of column; two Hermitian beam elements discussed in K. J. Bathe and S. model the column

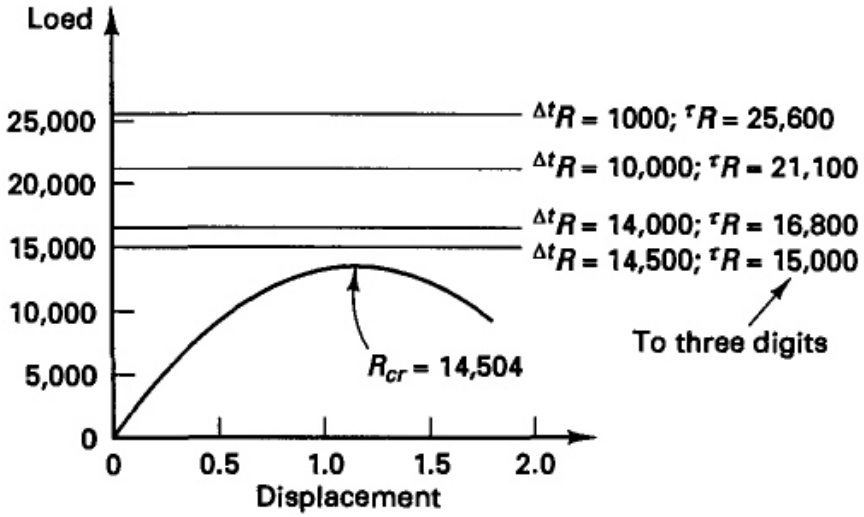

(b) Linearized buckling analysis of erch in Fig. E6.3; $L = 10$; $EA = 2.1 \times 10^6$

Figure 6.22 Linearized buckling analyses of two structures; in each case time t-Δt corresponds to time 0 (the unstressed state).

Analysis of arch

- Precollapse displacement are large.
- Linearized buckling analysis will give good result if the structure displays a column type of buckling behavior.

- Arch
- Ten two-node

isoparametric

beam element

Objectif:

Predict the collapse and postcollapse response

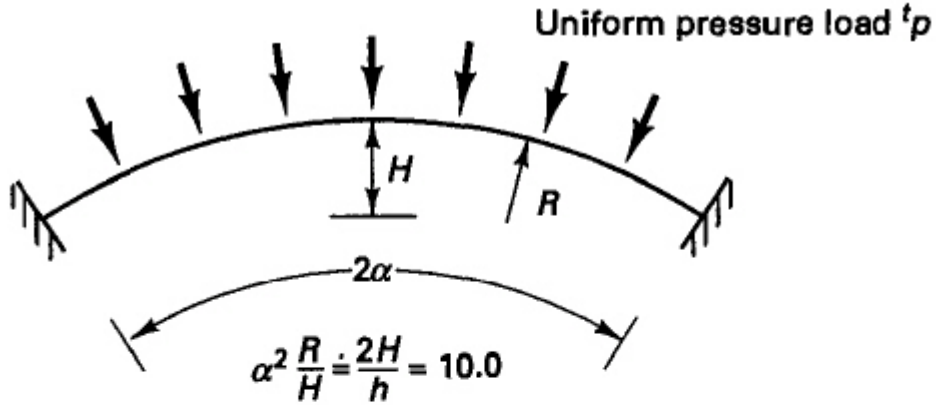

(a) Arch considered; ten 2-node isoparametric beam elements are used to model the complete structure

- Response calculated using a load-displacement-constraint method
- A linearized buckling analysis was performed using the state t-Δt the unstressed configuration and state Δt the configuration corresponding to a pressure of 10.

(a) Arch considered; ten 2-node isoparametric beam elements are used to model the complete structure

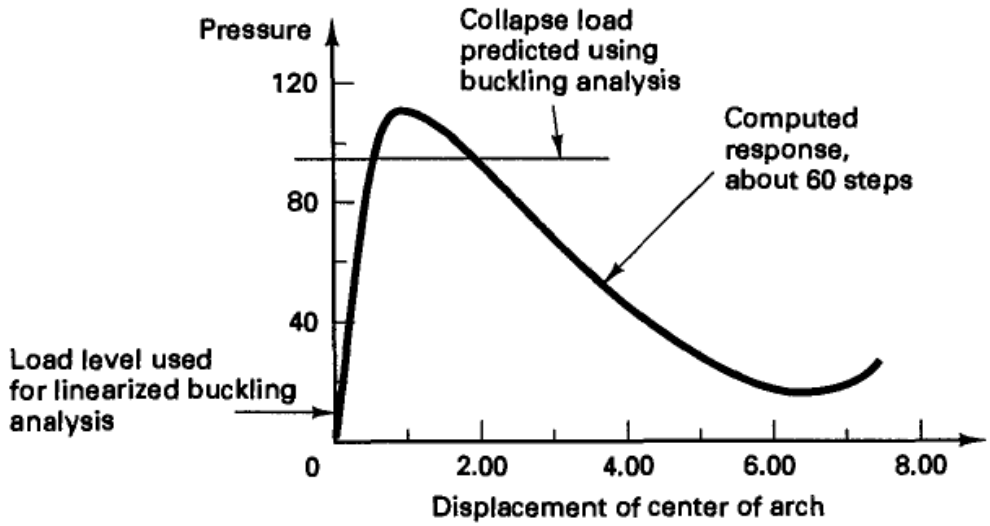

(b) Displacement response of perfectly symmetric structure

Figure 6.23 Collapse analysis of arch

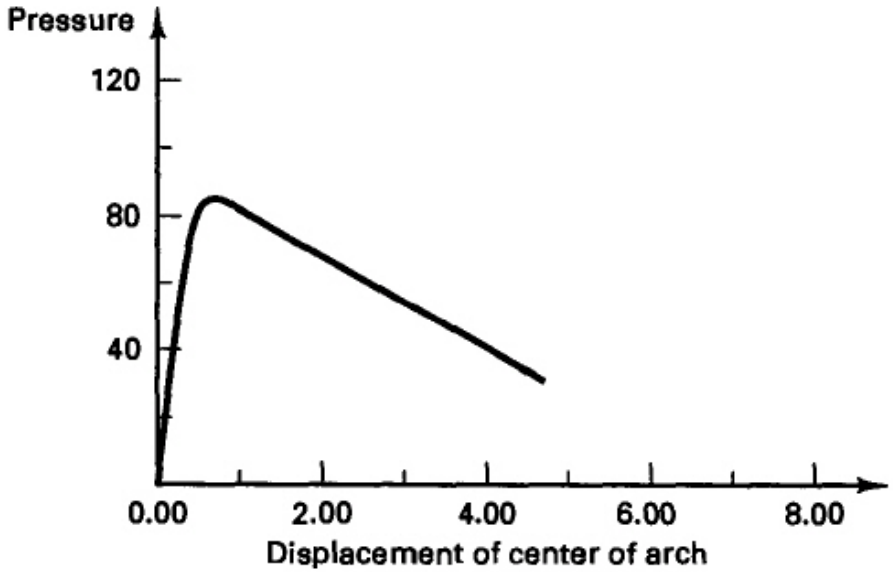

(d) Response of arch with antisymmetric imperfection

Figure 6.23 (*continued*)

Calculate response using a load displacement method with this geometric imperfection.
Pressure collapse load predicted is significantly smaller than the previous
The reduction is the collapse load is associated with a nonsymmetric behavior of the Structural model

Conclusion

- Structural imperfection can have a major effect on the predicted load-carrying capacity of a structure.
- Imperfection should be introduced in the structural model.
- Dynamic solution need to be considered, a dynamic buckling or collapse analysis that complete dynamic incremental analyses be performed for given different load levels.

6.8.3. The Effects of Elements Distortions

- In practice, element must largely be of a general straight-sided shapes with angular distortions in order to provide mesh grading and mesh complex geometries effectively.

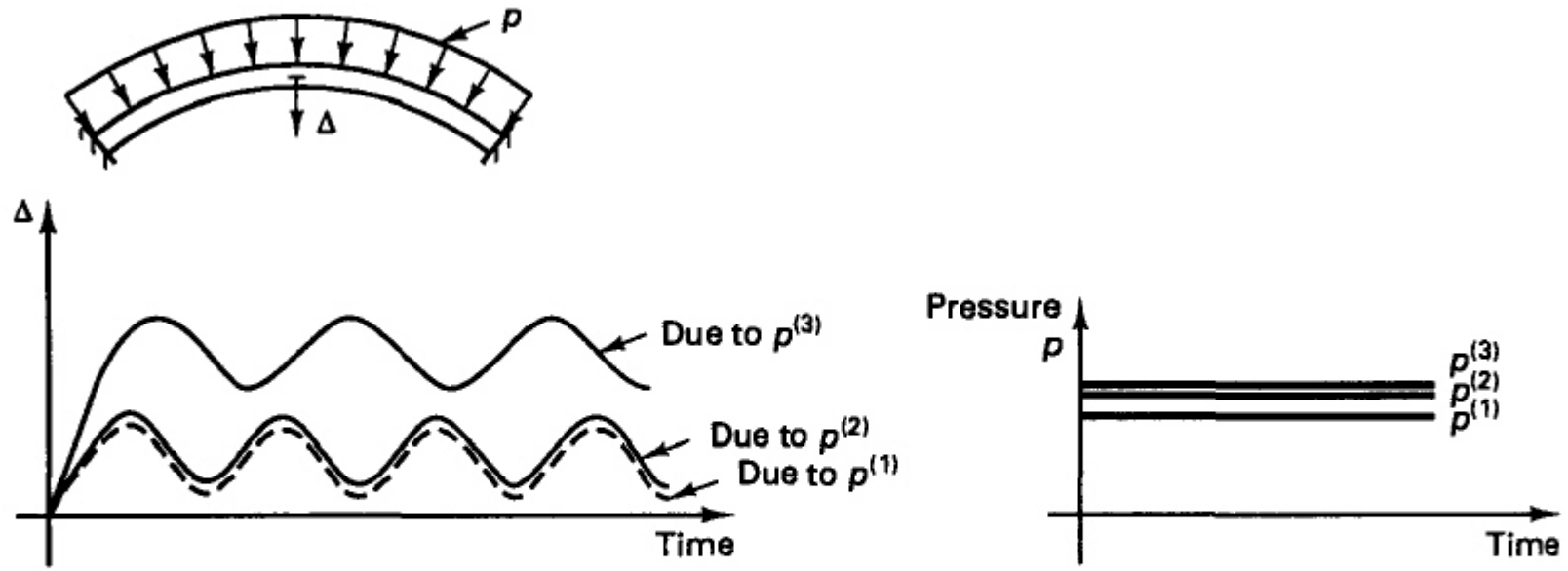

Figure 6.24 Dynamic buckling of arch; the structure shows a stable dynamic response due to load levels $p^{(1)}$ and $p^{(2)}$ and a much larger response due to $p^{(3)}$.

- In geometric nonlinear analysis significant angular and curved edge distortions due to non corner node element may arise a s consequence of deformation
- Using large displacement formulations, the principle of virtual displacement is applied to each element corresponding to the current configuration instead of the initial configuration in linear analysis.

6.8.4. The Effects of Order of Numerical Integration

- Nonlinear analysis : select appropriate numerical integration and order of integration.
- In geometric nonlinear analysis, at least the same integration order should be employed as linear analysis.
- An higher integration order than in the linear analysis may be required. This consideration is very important for beam, plate and shell.

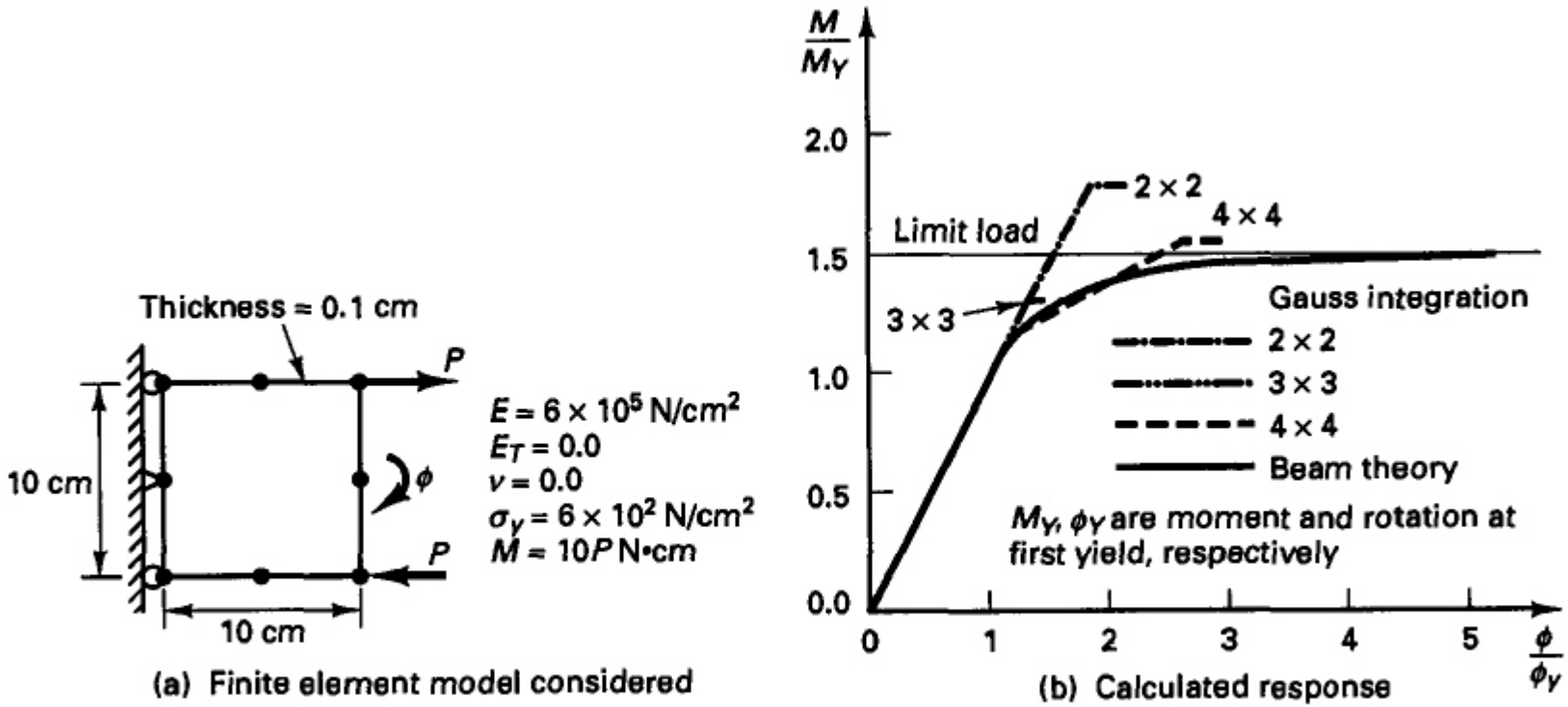

Figure 6.25 Effect of integration order in elastic-plastic analysis of beam section

Result using different order of Gauss integration for an eight-node plane stress representing the section of the beam.
Analyse illustrate that predict the nonlinear response accurately a higher Integration Order in the thickness direction beam is required than linear analysis.

EXAMPLE 6.24

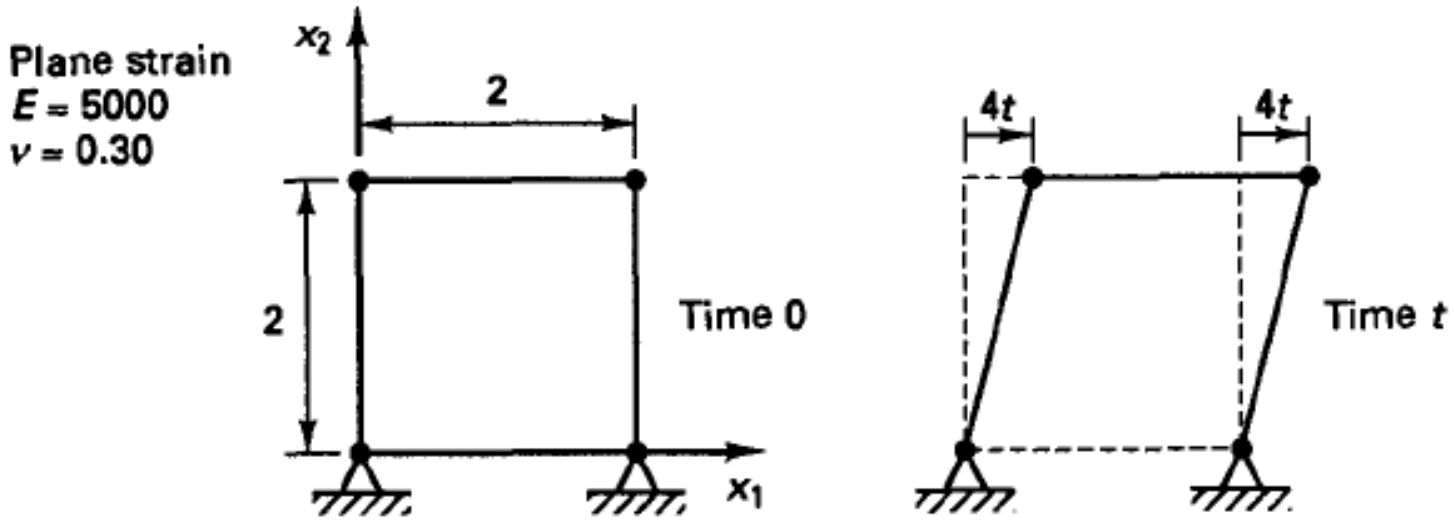

Figure E6.24 Four-node element subjected to motion

EXAMPLE 6.24: Consider the four-node element shown in Fig. E6.24. The displacements of the element are given as a function of time.

Calculate the Cauchy stresses using the following two stress measures:

(i) Use the *total formulation* of the second Piola-Kirchhoff stress and Green-Lagrange strain tensors,

$$ {}^{t}_{0}S_{ij} = {}^{t}_{0}C_{ijrs}\,{}^{t}_{0}\epsilon_{rs} \tag{a} $$

(ii) Use the *rate formulation* of the Jaumann stress rate and the velocity strain tensors (see L. E. Malvern [A]),

$$ {}^{t}\overset{\circ}{\tau}_{ij} = {}_{t}C_{ijrs}\,{}^{t}D_{rs} \tag{b} $$

(i) Use the *total formulation* of the second Piola-Kirchhoff stress and Green-Lagrange strain tensors,

$$ {}^{t}_{0}S_{ij} = {}^{t}_{0}C_{ijrs}\, {}^{t}_{0}\epsilon_{rs} \qquad \text{(a)} $$

Consider case (i). The deformation gradient is

$$ {}^{t}_{0}\mathbf{X} = \begin{bmatrix} 1 & 2t \\ 0 & 1 \end{bmatrix} $$

Let the Green-Lagrange strain tensor components at time t be given by

$$ {}^{t}_{0}\boldsymbol{\epsilon} = \tfrac{1}{2}({}^{t}_{0}\mathbf{X}^{T}\, {}^{t}_{0}\mathbf{X} - \mathbf{I}) $$

and hence,

$$ {}^{t}_{0}\boldsymbol{\epsilon} = \begin{bmatrix} 0 & t \\ t & 2t^{2} \end{bmatrix} $$

From table 4.2

Plane strain

$$\frac{E(1-\nu)}{(1+\nu)(1-2\nu)}\begin{bmatrix} 1 & \frac{\nu}{1-\nu} & 0 \\ \frac{\nu}{1-\nu} & 1 & 0 \\ 0 & 0 & \frac{1-2\nu}{2(1-\nu)} \end{bmatrix}$$

Plane strain
$E = 5000$
$\nu = 0.30$

Using Table 4.2 with the given values of E and ν, we obtain as nonzero values $C_{1111} = 6731$, $C_{2211} = C_{1122} = 2885$, $C_{2222} = 6731$, $C_{1212} = 1923$.

Hence, using the total Lagrangian description, we have

$${}^{t}_{0}S_{11} = 5770t^2; \qquad {}^{t}_{0}S_{22} = 13{,}462t^2; \qquad {}^{t}_{0}S_{12} = 3846t$$

$${}^{t}_{0}S_{ij} = {}^{t}_{0}C_{ijrs}\,{}^{t}_{0}\epsilon_{rs}$$

(ii) Use the *rate formulation* of the Jaumann stress rate and the velocity strain tensors (see L. E. Malvern [A]),

$$ {}^{t}\overset{\nabla}{\tau}_{ij} = {}_{t}C_{ijrs}\, {}^{t}D_{rs} \tag{b} $$

Next consider case (ii). The velocity strain tensor ${}^{t}\mathbf{D}$ is computed as given in (6.42). Hence,

$$ {}^{t}\mathbf{L} = \begin{bmatrix} 0 & 2 \\ 0 & 0 \end{bmatrix}; \qquad {}^{t}\mathbf{D} = \begin{bmatrix} 0 & 1 \\ 1 & 0 \end{bmatrix}; \qquad {}^{t}\mathbf{W} = \begin{bmatrix} 0 & +1 \\ -1 & 0 \end{bmatrix} $$

Now we use the same constitutive matrix $\mathbf{C}$ to obtain

$$ \begin{bmatrix} {}^{t}\overset{\nabla}{\tau}_{11} \\ {}^{t}\overset{\nabla}{\tau}_{22} \\ {}^{t}\overset{\nabla}{\tau}_{12} \end{bmatrix} = \begin{bmatrix} 0 \\ 0 \\ 3846 \end{bmatrix} $$

We note that the Jaumann stress rate is independent of time. However, the material also rotates as expressed in ${}^{t}\mathbf{W}$ and the time rates of the Cauchy stress components are given by

$$ \begin{bmatrix} {}^{t}\dot{\tau}_{11} \\ {}^{t}\dot{\tau}_{22} \\ {}^{t}\dot{\tau}_{12} \end{bmatrix} = \begin{bmatrix} 2\,{}^{t}\tau_{12} \\ -2\,{}^{t}\tau_{12} \\ 3846 + {}^{t}\tau_{22} - {}^{t}\tau_{11} \end{bmatrix} $$

These differential equations can be solved to obtain (again to two significant figures and hence using $G = \dfrac{E}{2(1+\nu)} \doteq 1900$)

$$ \begin{bmatrix} {}^{t}\tau_{11} \\ {}^{t}\tau_{22} \\ {}^{t}\tau_{12} \end{bmatrix} = \begin{bmatrix} 1900(1 - \cos 2t) \\ -1900(1 - \cos 2t) \\ 1900 \sin 2t \end{bmatrix} \tag{d} $$

We note that the results given in (c) and (d) are quite different when t is larger than about 0.1 and that in each material description normal stresses are generated (that are zero when infinitesimally small strains are assumed). Also, the oscillatory behavior of the Cauchy stresses in (d) with period π is peculiar.

EXAMPLE 6.27: Consider element 2 in Example 4.5 and assume that in an elastoplastic analysis the stresses at time t in the element are such that the tangent moduli of the material are equal to $E/100$ for $0 \leq x \leq 40$ and equal to E for $40 < x \leq 80$ as illustrated in Fig. E6.27. Evaluate the tangent stiffness matrix ${}^t\mathbf{K}$ using one-, two-, three-, and four-point Gauss integration and compare these results with the exact stiffness matrix. Consider only material nonlinearities.

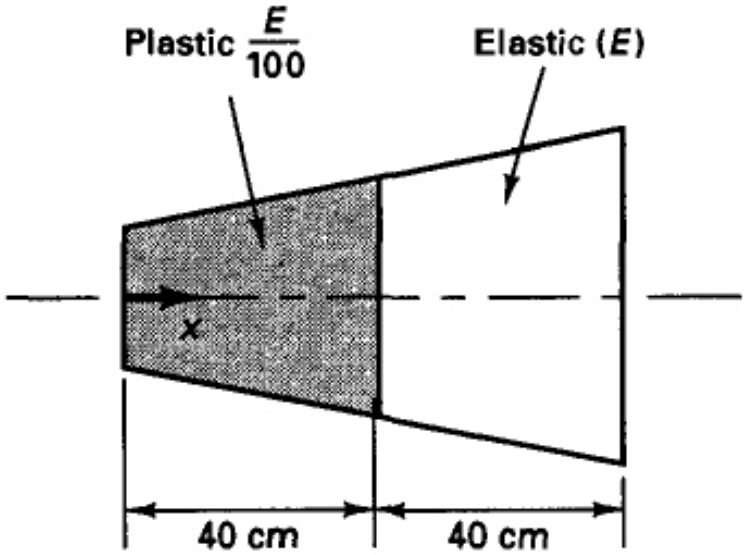

Figure E6.27 Element 2 of Example 4.5 in elastic-plastic conditions

For the evaluation of the matrix ${}^{1}\mathbf{K}$ we use the information given in Example 4.5 and in Table 5.6. Thus, we obtain the following results:

One-point integration:

$$ {}^{1}\mathbf{K} = 2 \times 40 \begin{bmatrix} -\frac{1}{80} \\ \frac{1}{80} \end{bmatrix} \frac{E}{100} \begin{bmatrix} -\frac{1}{80} & \frac{1}{80} \end{bmatrix} (1 + 1)^2 = 0.0005E \begin{bmatrix} 1 & -1 \\ -1 & 1 \end{bmatrix} $$

Two-point integration:

$$ {}^{1}\mathbf{K} = 1 \times 40 \begin{bmatrix} -\frac{1}{80} \\ \frac{1}{80} \end{bmatrix} \frac{E}{100} \begin{bmatrix} -\frac{1}{80} & \frac{1}{80} \end{bmatrix} \left(1 + 1 - \frac{1}{\sqrt{3}}\right)^2 $$

$$ + 1 \times 40 \begin{bmatrix} -\frac{1}{80} \\ \frac{1}{80} \end{bmatrix} E \begin{bmatrix} -\frac{1}{80} & \frac{1}{80} \end{bmatrix} \left(1 + 1 + \frac{1}{\sqrt{3}}\right)^2 $$

$$ = 0.04164E \begin{bmatrix} 1 & -1 \\ -1 & 1 \end{bmatrix} $$

Three-point integration:

$$
{}^{t}\mathbf{K} = \frac{5}{9}40\begin{bmatrix} -\frac{1}{80} \\ \frac{1}{80} \end{bmatrix}\frac{E}{100}\begin{bmatrix} -\frac{1}{80} & \frac{1}{80} \end{bmatrix}\left(1 + 1 - \frac{\sqrt{3}}{5}\right)^2
$$

$$
+ \frac{8}{9}40\begin{bmatrix} -\frac{1}{80} \\ \frac{1}{80} \end{bmatrix}\frac{E}{100}\begin{bmatrix} -\frac{1}{80} & \frac{1}{80} \end{bmatrix}(1 + 1)^2
$$

$$
+ \frac{5}{9}40\begin{bmatrix} -\frac{1}{80} \\ \frac{1}{80} \end{bmatrix}E\begin{bmatrix} -\frac{1}{80} & \frac{1}{80} \end{bmatrix}(1 + 1 + \sqrt{3}/5)^2
$$

$$
{}^{t}\mathbf{K} = 0.02700E\begin{bmatrix} 1 & -1 \\ -1 & 1 \end{bmatrix}
$$

Four-point integration:

	r_i	α_i
$n = 4$	$\pm 0.8611\ldots$	$0.3478\ldots$
	$\pm 0.3399\ldots$	$0.6521\ldots$

$$
{}^{t}\mathbf{K} = 0.3478\ldots(40)\begin{bmatrix} -\frac{1}{80} \\ \frac{1}{80} \end{bmatrix}\frac{E}{100}\begin{bmatrix} -\frac{1}{80} & \frac{1}{80} \end{bmatrix}(1 + 1 - 0.8611\ldots)^2
$$

$$
+ \ldots
$$

$$
{}^{t}\mathbf{K} = 0.04026E\begin{bmatrix} 1 & -1 \\ -1 & 1 \end{bmatrix}
$$

The exact stiffness matrix is

$$
{}^{t}\mathbf{K} = \begin{bmatrix} -\frac{1}{80} \\ \frac{1}{80} \end{bmatrix} \frac{E}{100} \begin{bmatrix} -\frac{1}{80} & \frac{1}{80} \end{bmatrix} \left\{ \int_0^{40} \left(1 + \frac{y}{40}\right)^2 dy + \int_{40}^{80} 100 \left(1 + \frac{y}{40}\right)^2 dy \right\}
$$

$$
= \begin{bmatrix} -\frac{1}{80} \\ \frac{1}{80} \end{bmatrix} E \begin{bmatrix} -\frac{1}{80} & \frac{1}{80} \end{bmatrix} \left\{ \frac{40}{300} \left(1 + \frac{y}{40}\right)^3 \Big|_0^{40} + \frac{40}{3} \left(1 + \frac{y}{40}\right)^3 \Big|_{40}^{80} \right\}
$$

$$
{}^{t}\mathbf{K} = 0.03973E \begin{bmatrix} 1 & -1 \\ -1 & 1 \end{bmatrix}
$$

It is interesting to note that in this case the two-point integration yields more accurate results than the three-point integration and that a good approximation to the exact stiffness matrix is obtained using four-point integration.